Experimental study on remaining tensile strength of wide steel specimens with different corrosion conditions

Tatsumasa KAITA*, Hiroyuki IKEDA**, J.M.R.S. Appuhamy***, Mitao OHGA****, Katashi FUJII*****

* Assistant Professor, Department of Civil Engineering and Architecture, Tokuyama College of Technology, JAPAN

** Graduate student, Department of Civil and Environmental Engineering, Graduate School of Science and Engineering, Ehime University, JAPAN

*** Doctoral student, Department of Civil and Environmental Engineering, Graduate School of Science and Engineering, Ehime University, JAPAN

**** Professor, Department of Civil and Environmental Engineering, Graduate School of Science and Engineering, Ehime University, JAPAN

***** Professor, Department of Social and Environmental Engineering, Graduate School of Engineering, Hiroshima University, JAPAN

ABSTRACT: In recent years, the maintenance techniques in steel bridge management system have been becoming more and more serious problem in Japan. This paper presents more accurate remaining strength estimation method for tensile corroded members. For this purpose, the tensile test and steel surface measurement of severe corroded specimens were carried out in this study. Most important features of this tensile test are that all 26 specimens have wide width (70-180 mm: actual member size) and totally different corroded conditions. The 3-dimensional scanning system had been applied to steel surface measurement in order to investigate the relationship between the remaining strength and statistical features of surface irregularities. From the experimental results, main conclusions of this study are follows:

(1) Influence of stress concentration due to surface irregularities appear clearly around yield load stage.

(2) A minimum thickness (t_{min}) and its position are very important to estimate the remaining tensile strength.

(3) A simple estimation method, which used a new statistical parameter t_{min}/t_0 (t_0: original thickness), was proposed for the remaining tensile strength of corroded plate members.

KEYWORDS: Corrosion, Strength estimation, Minimum thickness, Yielding, Breaking

1. INTRODUCTION

In recent years, maintenance of corroded steel bridges has been becoming widely-recognized as one of the most important tasks in bridge management system, through some breaking accident reports of corroded members on in-service bridges (Fujino et al. (2008)). Since the corrosion will deteriorate their performance with time, whether or not the corroded structures have enough redundancy for the failure should be correctly judged in bridge maintenance system. Therefore, more accurate remaining strength estimation method, and the thickness measurement technique, which is applicable to on-site measurement, would be essential as core part of corroded structure maintenance. Some loading tests

of corroded steel plates under tensile force were carried out in past studies. Matsumoto et al. (1992) investigated tensile strength, using tensile coupon specimens with corrosion. In order to estimate the remaining tensile strength of a corroded plate, they proposed a representative thickness as the minimum value of average thickness of the cross-section perpendicular to loading axis. And, Muranaka et al. (1998) proposed representative thickness $t_z = t_{avg} - 0.7\sigma_t$ (t_{avg}: average thickness, σ_t: standard deviation of thickness) for the estimation of tensile strength and fatigue strength.

However, since widths of their test specimens are very small (less than 30mm), the influence which the corroded conditions give the remaining strength estimation will be difficult to comprehend. For an example of this fact, a lot of corrosion pits with more than 30mm diameters are existing in actual corroded members. Due to this reason, it would be required using the specimens with actual steel member size for obtaining more reliable experimental results.

Therefore, this paper presents a simple remaining strength estimation method, which based on the loading tests by using widely plate specimens, with high accuracy for tensile corroded members. Moreover, the relationship between the statistical parameters of plates and the remaining strength, yield and ultimate processes and breaking positions were investigated through the surface measurement.

The varied corrosion conditions due to severe corrosion were categorized into 3 typical corrosion types based on the consideration of surface measurement results.

2. SEVERE CORRODED TEST SPECIMENS

26 specimens for the tensile test were cut out from a corroded plate girder, which had been used for about a hundred years at Ananai River in Kochi prefecture, for the tensile test. This plate girder was constructed
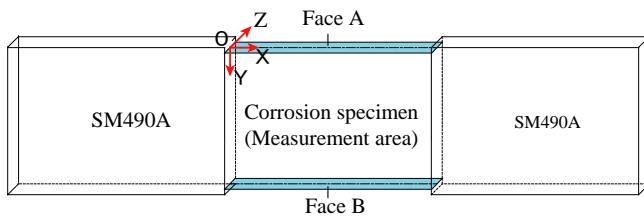

(a) Flange specimen

(b) Web specimen
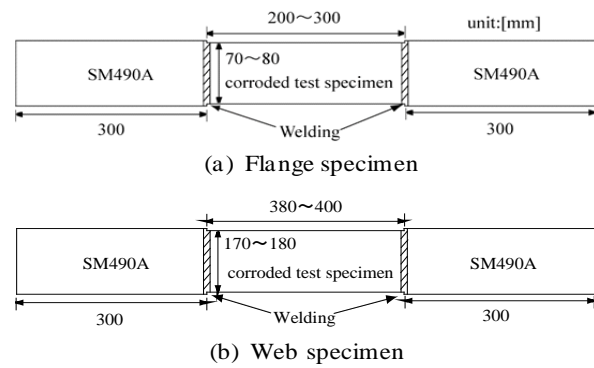
Figure1. Dimensions of test specimens

Table1. Material properties

Specimens	Flange	Web
Elastic modulus [GPa]	187.8	195.4
Poisson's ratio	0.271	0.281
Yield stress [MPa]	281.6	307.8
Tensile strength [MPa]	431.3	463.5
Elongation at breaking [%]	40.19	32.87

by using rivet joint, and had been exposed to strong salty wind from the Pacific Ocean. Test specimens were cut out from the cover plate on upper flange (Initial thickness=10.5mm) and web (Initial thickness=10.0mm) plate. Many severe corrosion damages distributed all over the girder, especially, large corrosion pits or locally-corroded portions were observed on upper flanges and its cover plates.

Before the measurement of steel surface, all specimens had been fabricated as shown in Figure 1. All rusts over both surfaces were removed carefully by using the electric wire brushes and punches. Two new SM490A plates (t=16mm) were jointed to both sides of specimen by the butt full penetration welding for grip parts to loading machine, as shown in **Figure1**. Here, the flange and web specimens have the widths ranged from 70-80mm and 170-180mm, respectively. 21 flange specimens (F1-F21) and 5 web specimens (W1-W5) were fabricated for tensile test.

In addition, 4 corrosion-free specimens (JIS5 type) were made from flange and web each two, and tensile tests were carried out to clarify the material properties of test specimens. **Table1** shows the material properties obtained from these test results.

Figure2. Coordinate system for measurement

Photo1. Surface measurement situation

Table2. Measurement and categorization results of all test specimens

Specimens	Average corrosion depth C_{avg} [mm]	Standard deviation σ_t [mm]	Corrosion type
F-1	1.444	1.137	Pitting
F-2	0.423	0.243	Overall
F-3	1.230	0.692	Pitting
F-4	0.434	0.231	Overall
F-5	2.718	1.314	Pitting
F-6	0.953	0.419	Overall
F-7	0.635	0.396	Overall
F-8	0.277	0.237	Overall
F-9	0.581	0.593	Pitting
F-10	3.781	2.362	Local
F-11	2.453	1.552	Pitting
F-12	1.254	0.753	Pitting
F-13	0.803	0.706	Pitting
F-14	0.413	0.248	Overall
F-15	1.292	1.010	Pitting
F-16	0.437	0.364	Overall
F-17	1.333	1.442	Pitting
F-18	1.914	1.409	Pitting
F-19	0.989	1.568	Local
F-20	3.421	1.864	Local
F-21	0.412	0.252	Overall
W-1	0.495	0.407	Overall
W-2	0.430	0.239	Overall
W-3	0.356	0.213	Overall
W-4	0.623	0.225	Overall
W-5	0.503	0.309	Overall

3. CORROSION SURFACE MEASUREMENT

3.1 Measurement method

The measurement area and coordinate system are shown in **Figure2**. The measuring device has three arms and six rotational joints, and can measure the coordinates of a point on steel surface by using the non-contact scanning probe (laser line probe). Before the measurement, the global coordinate system with an original point on Face A was set, as shown in **Figure2**. The advantage of this device is that the coordinate values of arbitrary surface point can be given by using the coordinate system set up initially, even if the device is moved to other position from the initial position.

The situation of measurement using the scanning probe is shown in **Photo1**. Since this probe irradiates the steel surface with a laser beam, which has about 100mm width, the large number of 3-dimensional coordinate data can be obtained easily at a time.

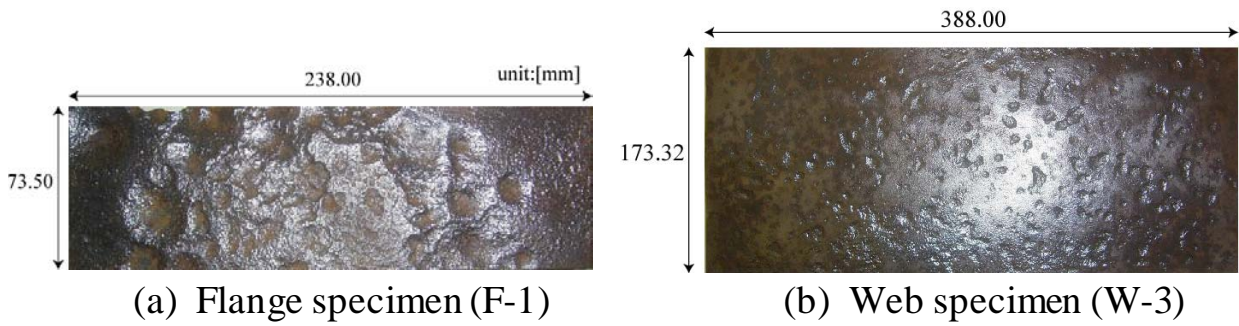In this measurement, the 3-dimensional coordinate data is obtained as many in-line dot data. The intervals of dot data in a laser-line are less than about 0.1mm, and the laser-line intervals are about 0.5~1.0 mm. The number of measured data in one-surface of one specimen is about five hundred thousand.

In order to obtain the remaining thickness of each specimen and to perform statistical processing such as calculation of average thickness and expression of thickness histogram etc., it is necessary to give the coordinate values for square grid points with equal intervals. From consideration of above mentioned fact, the coordinate data was adjusted to grid data with 0.5mm intervals in the flange surface. And the remaining thickness of all grid points was calculated by using the difference of the coordinate values for both sides of corroded specimens.
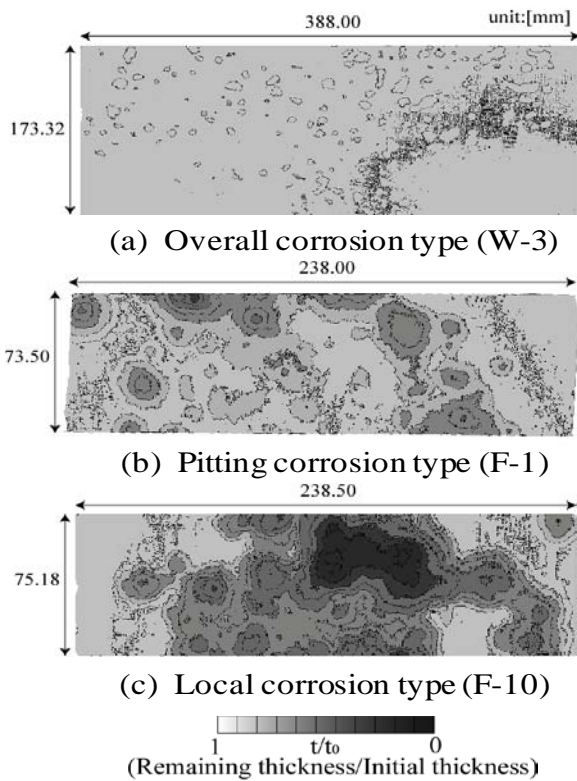
3.2 Measurement results

3.2.1 Features of corroded surface

The measurement results of corrosion surface irregularity are shown in **Table2**. It is clarified that the corrosion progress of flange specimens is more severe than it of web specimens from the average

(a) Flange specimen (F-1)   (b) Web specimen (W-3)

Photo2. Examples of corroded surface

(a) Overall corrosion type (W-3)

(b) Pitting corrosion type (F-1)

(c) Local corrosion type (F-10)

1   t/t_0 0
(Remaining thickness/Initial thickness)

Figure3. Contour map of 3 corrosion types

thickness.

Photo2 shows the example specimens with typical corrosion types of flange and web specimens respectively. In **Photo2** (a), many large corrosion pits (pitting corrosion) with about 10-50mm diameters are existed on only one surface. Furthermore, severely corroded portions were observed in constant intervals (every 60cm) on flange plate. The reason will be influence of the boundary corrosion between railroad tie and steel surface. On the other hand, for web specimen, some small corrosion pit (less than 10mm diameters) were scattered on plate surface, because the salty wind will remain to inside of main girders. The large

standard deviation of thickness (σ_t) shows the corrosion type with large irregularities such as flange specimen (F-1).

3.2.2 Categorization of corrosion conditions

It will be necessary that the varied corrosion condition, which may appear in actual steel structures, should be categorized to few typical corrosion types for estimation method with generality. In this study, based on the results of measurement of corrosion surface irregularity, all specimens were categorized into typical 3 corrosion types (**Figure3** and **4**), concerning standard deviation of thickness and corrosion conditions, as follows:
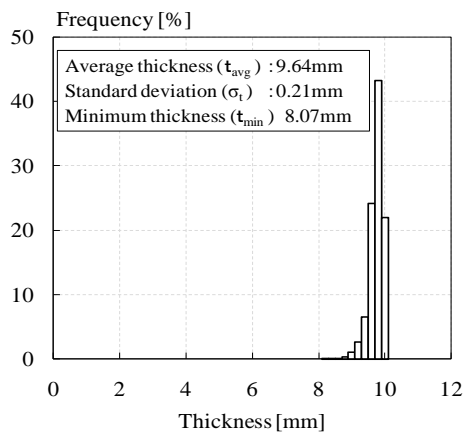
(1) Overall corrosion type (Type-O)

In this corrosion type, the small corrosion pits or minor corrosion was spread on all over the plate surface. And, σ_t becomes also comparatively small value (σ_t is about less than 0.50mm).
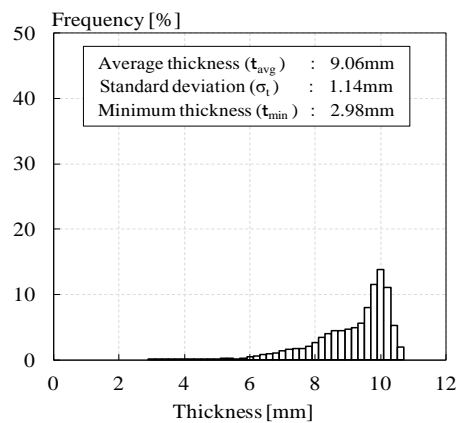
From **Figure3** (a), although small corrosion pits are distributed over a surface, corrosion progress seems extremely slight. In this corrosion type, the peak of thickness histogram is almost the same to average thickness, and the distribution width of thickness is very narrow.
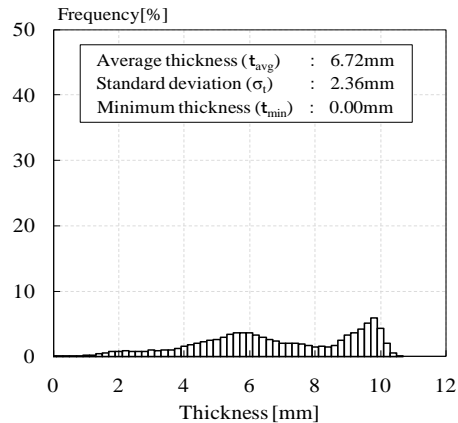
(2) Pitting corrosion type (Type-P)

This corrosion surface, which has the σ_t in the range of about 0.50mm< σ_t <1.80mm, must have some large corrosion pits (more than 20mm diameters). Namely, this corrosion type will be able to consider that the corroded state is more progressed by any reasons than overall corrosion type. From **Figure3**

Frequency [%]

Average thickness (t_{avg}) : 9.64mm
Standard deviation (σ_t) : 0.21mm
Minimum thickness (t_{min}) 8.07mm

Thickness [mm]

(a) Overall corrosion type (W-3)

Frequency [%]

Average thickness (t_{avg}) : 9.06mm
Standard deviation (σ_t) : 1.14mm
Minimum thickness (t_{min}) : 2.98mm

Thickness [mm]

(b) Pitting corrosion type (F-1)

Frequency[%]

Average thickness (t_{avg}) : 6.72mm
Standard deviation (σ_t) : 2.36mm
Minimum thickness (t_{min}) : 0.00mm

Thickness [mm]

(c) Local corrosion type (F-10)
Figure4. Thickness histogram of
3 corrosion types

(b), it is characteristic that although the severe corroded portions due to large corrosion pits exist in some places, almost non corroded portions also remain widely. In **Figure4** (b), it can be noticed that the distribution width of thickness is larger than that of overall corrosion type, and the peak of histogram is not same to average thickness.

(3) Local corrosion type (Type-L)

When the corrosion progresses than pitting corrosion types, some large corrosion pits will overlap continuously each other. And more severe corroded portion will form such as F-10 shown as **Figure3** (c). In this paper, an ultimate state of corrosion with large area like this **Figure3** (c) is called "Local corrosion type". This corrosion type may cause the through-hole on the plate such as F-10, if it was neglected for long term. From the histogram as shown in **Figure4** (c), local corrosion type has few peaks in thickness histogram, and highest peak will differ widely to average thickness. In other words, this fact means that the average thickness will not be able to apply as representative thickness for strength estimation method of tensile corroded members.

Categorized corrosion type of all test specimens are also shown in **Table2**. Here, Overall: Overall corrosion type, Pitting: Pitting corrosion type and Local: Local corrosion type, respectively.

In this study, a simple remaining strength method, which is considered statistical features mentioned above and categorized corrosion type, by using a new effective thickness including any representative thicknesses will be discussed after loading test. And not only the remaining strength but also each yielding process, ultimate mechanic behaviors and breaking positions will be investigated through the loading test.

4. TENSILE LOADING TEST

4.1 Loading condition and measuring equipments

Tensile loading tests were carried out at constant velocity under loading control by using a hydraulic loading test machine (maximum load: 2940KN). The loading velocity was set to 150N/sec for severe corrosion specimen such as Type-P or L, and the other specimens have about 200N/sec loading velocity.
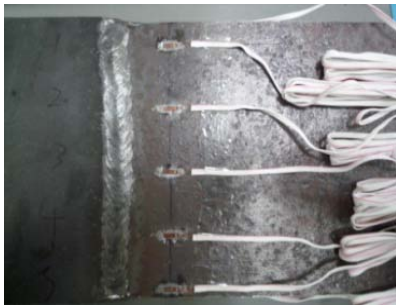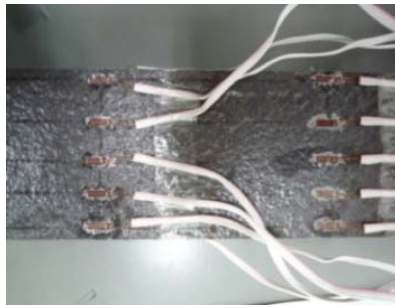
| (a) Overall corrosion type (W-3) | (b) Pitting corrosion type (F-1) | (c) Local corrosion type (F-10) |

Photo3. Strain gauges

Table3. Results of tensile test

Specimens	Yield strength P_y [kN]	Tensile strength P_b [kN]	Effective thickness t_{e_y} [mm]	Effective thickness t_{e_b} [mm]
F-1	167.24	224.26	8.08	7.07
F-3	186.81	289.32	8.51	8.61
F-5	143.59	196.53	6.99	6.24
F-10	73.84	80.48	3.49	2.48
F-11	147.24	203.78	6.81	6.16
F-13	192.79	273.54	8.75	8.11
F-17	154.90	219.00	7.07	6.53
F-18	137.49	190.26	6.47	5.84
F-20	104.10	131.66	4.89	4.04
W-3	497.69	735.69	9.33	9.15
W-5	498.37	663.91	9.12	8.07

In tensile tests, the number and position of strain gauges are differing in each specimen, because the corroded conditions are considered. 3 examples of corroded specimen with some strain gauges are shown in **Photo3**. In **Photo3** (a), the strain gauges of Type-O are set on a minimum section because it is obvious that stress concentration and breaking will occurred in the immediate vicinity of this section. And intervals of gauges are comparatively sparse.

Type-P and L specimens have many strain gauges than Type-O specimens, as shown in **Photo3** (b) and (c). More attention was paid on both a minimum section and local portions with serious corrosion damage in these specimens. Therefore, the strain gauges were set closely on their both surfaces in order to clarify the stress and strain distributions at each load stages. The intervals of strain gauges were decided by considering the surface condition.

The elongations at maximum load and after breaking were calculated by measuring the distance between some gauge points at backward and forward of each focused section. Here, the distance between the gauge points in before the tensile tests is 100mm.

The vertical displacements of jacks were measured by laser displacement gauge. In this study, since the slip between jacks and specimen can be observed, the vertical displacement of jacks was assumed as that of specimen.

4.2 Experimental results and discussions

At the present time, the loading tests had been finished about 11 specimens (9 flange and 2 web specimens) with more severe corroded conditions.
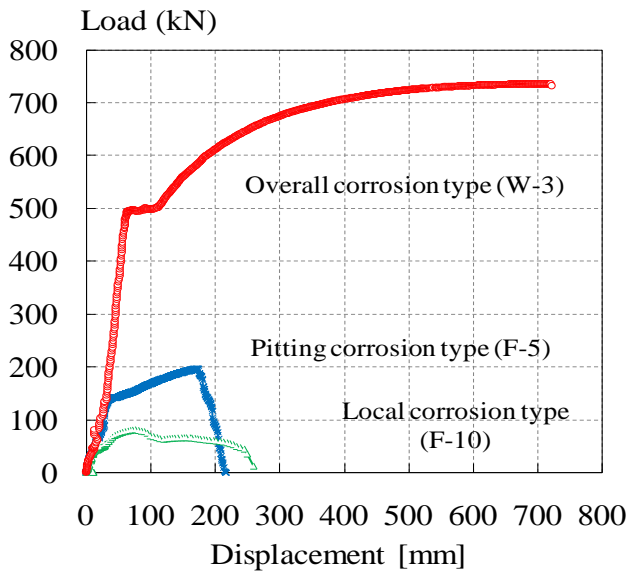
Figure5. Load-displacement curves

4.2.1 Remaining yield and tensile strength

The experimental results of tensile tests of corroded specimens are shown in **Table3**.

An effective thickness (t_{e_y} and t_{e_b}) of **Table3** is expressed in following equations:

$$t_{e\_y} = \frac{P_y}{B \times \sigma_y} \qquad (3.1)$$

$$t_{e\_b} = \frac{P_b}{B \times \sigma_b} \qquad (3.2)$$

Here, P_y and P_b: yield and tensile (maximum) load, σ_y and σ_b: yield and tensile stress, and B: width of specimens.

4.2.2 Yielding process and Ultimate behaviors

Figure5 shows an example of load-displacement curves of 3 corrosion types. It was found that a curve of Type-O specimen (W-3) is almost the same as the general corrosion-free specimens, and yield load is also confirmed clearly at the vicinity of 500kN. This result will indicate that the yield process and ultimate behaviors may be dominated by an averaged thickness parameter of all over the plate, when the plate has overall corrosion.

On the other hand, although the yield load of Type-P specimen (F-1) can be observed by difference of curve inclinations at about 150kN, the increase of displacement at yield load cannot found. As this

reason, it will be thought that the yield began slowly from some points of pitting corrosion at 150kN, and the yield regions would progress linearly with displacement to maximum load. Moreover, it can be noticed that the breaking load is remarkably small, because the crack progressed gradually after maximum load. And, the vertical displacement at yield and maximum load are deteriorated than that of Type-O. This fact will show that the entire elongation of specimen with serious corrosion damages becomes small, because only local portion in corrosion pits will be elongate due to stress concentration.

For the Type-L specimen (F-10), the features mentioned above appear dominantly than Type-P. Especially, yield loads of all Type-L specimens could not be found from load-displacement curves. The yield strength of this type was judged from the comparison between the measured strain value and a yield strain.

An example of strain distributions of Type-P specimen (F-17) is shown in **Figure6**. These strains were measured by the minimum section of specimen. And **Figure7** shows the thickness contour map of F-17. **Figure6** (a) and (b) show the strain distribution before and after the yield load, respectively. In these figures, the yield strain (1500$\mu\varepsilon$), which was obtained by tensile tests of corrosion-free specimens, is also indicated as a red line. And the yield load was observed about 155.8kN from the load-displacement relationship.

In **Figure6** (a), the distribution of strain is almost constant under 100kN. After that, the strain near the large corrosion pit begins to appear a tendency to increase from 140kN in comparison with both ends, but the difference is very small. And in P=151.42kN, the strain of plate center (3) was over a yield strain, and then the strains (2) and (4) were yielded successively to yield load. These facts show that plastic region spreads out drastically from a center

(a) Before yield

(b) After yield
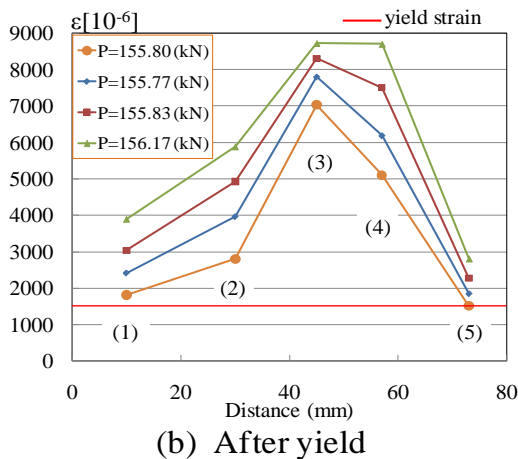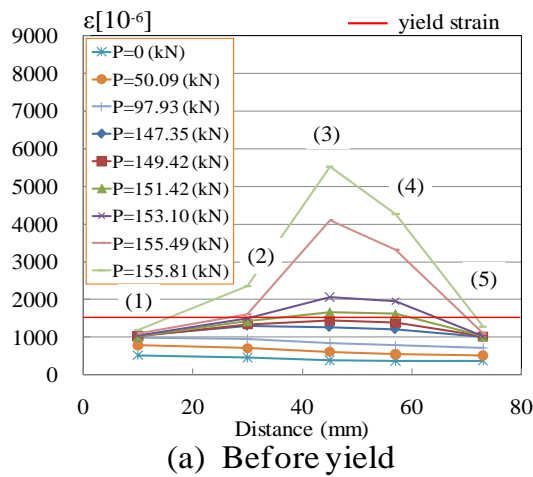
Figure6. Strain distributions (F-17)

(Remaining thickness/Initial thickness)
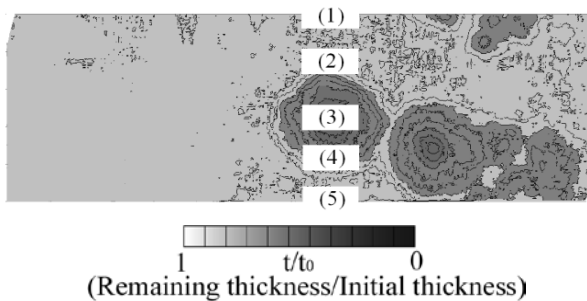
Figure7. Thickness contour map of F-17

part of corrosion pits to both sides. After the yield load, all strain values increase with the load at almost constant rate, as shown in **Figure6** (b).

From these results, the influence of stress concentration cannot be confirmed at initial load stage (elastic state), and that will appear significantly at the vicinity of yield load stage.

4.2.3 Breaking behavior

The breaking states of Type-P specimen (F-1) are shown in **Photo4**. In **Photo4** (a), crack occurred at a

(a) Crack occurring (b) Crack progressing

Photo4. Breaking state

minimum thickness point (left side of specimen in **Photo4** (a)). At this time, crack occurring means that the remaining strength reaches the maximum load, and then the load will begin to deteriorate rapidly. After that, crack progresses to right angle direction of load axis, depending on the surface irregularities (**Photo4** (b)). This phenomenon will be able to confirm from the deterioration of breaking load in **Figure5**.

Breaking state mentioned above is clearly different from the results of past tensile test by using coupon specimens such as JIS5 type specimens. Namely, in the case of coupon specimens with narrow width, there is little breaking case due to the crack at minimum thickness point. (Tagaya et al. 2005) Instead, breaking state of coupon specimen will be close to a ductile breaking, which has large breaking load, such as corrosion-free plate than the experimental results of wide specimen in this study.

Thus, these facts mean that it will be very important to predict a breaking trigger point from thickness measurement results for more accurate tensile strength estimation method in order to apply to actual steel structure maintenance.

### 4.2.4 Consideration for breaking trigger point

Distribution diagrams of maximum thickness, average thickness and minimum thickness in longitudinal axis direction are shown in **Figure8**.

In the case of Type-O, the roughness of thickness distribution is very small (**Figure8** (a)). And the relationship between the breaking position and each thickness distribution will not clarify, but it may
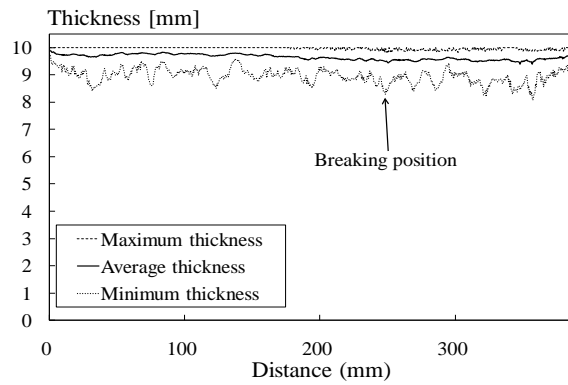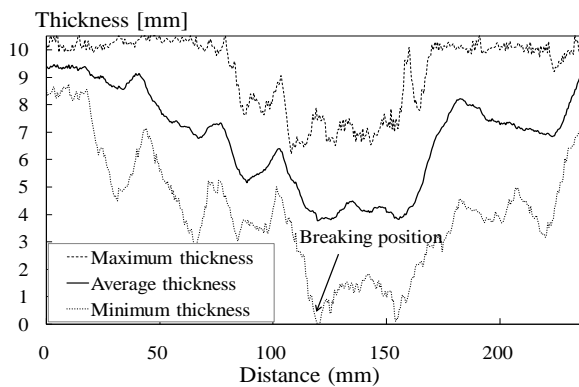
(a) Type-O (W-3)
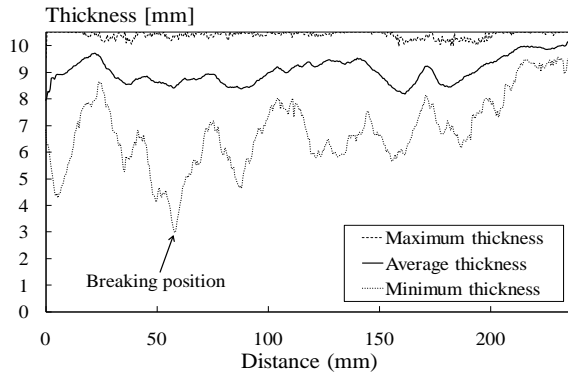
(b) Type-P (F-1)

(c) Type-L (F-10)

Figure8. Thickness distribution

seem that the breaking position corresponds to a minimum section (the minimum peak of average thickness) and minimum thickness point. Thus, the breaking trigger point of Type-O may be dominated to a thickness of the minimum section at right angle to the load axis.

However, it can be confirmed that Type-P and L specimens break at the section including the minimum thickness point independently of the average thickness, as shown in **Figure8** (b) and (c). This analytical result shows that the stress concentration at minimum thickness point due to

local corrosion damages will affect to crack occurrence in ultimate state and the remaining strength of steel plates subjected to tensile force.

Finally, the minimum value of average thickness on a section at right angle to load axis (t_{avg_min}) should be paid attention to the accurate remaining strength of corroded plates with overall corrosion surface. Moreover, as a new concept of strength estimation, it should be focused attention on the remaining minimum thickness and its position as one of the breaking trigger. In addition, if minimum thickness position and minimum section exist in a same section, it goes without saying that its section must become a breaking trigger.

## 5. REMAINING STRENGTH ESTIMATION

5.1 Yield strength estimation

An effective thickness (Equation (3.1) and (3.2)) concept is more commonly used for remaining strength estimation method of corroded plates as it is simple and useful. But the effective thickness cannot be obtained from in-service steel structures. The measurable statistical thickness parameter, which has a high correlation with the effective thickness as shown in **Table3**, was investigated in this section.

The correlation diagrams between an effective thickness of yield strength and 4 statistical thickness parameters (t_{avg}, t_{min}, t_{avg_min} and t_z) are shown in **Figure9**. From **Figure9** (a), the average thickness tends to become larger than effective thickness, because the influence of stress concentration due to corrosion will not able to consider carefully. Therefore, the strength estimation using only t_{avg} will overestimate the remaining yield strength. On the other hand, it can be found that the yield strength estimation using t_{min} will provide considerably underestimated results, as shown in **Figure9** (b). **Figure9** (c) shows the estimation results by using thickness parameter $t_z = t_{avg} - 0.7\sigma_t$, which had been
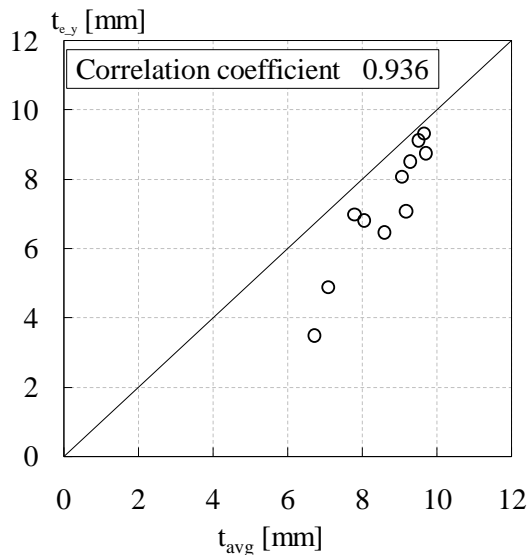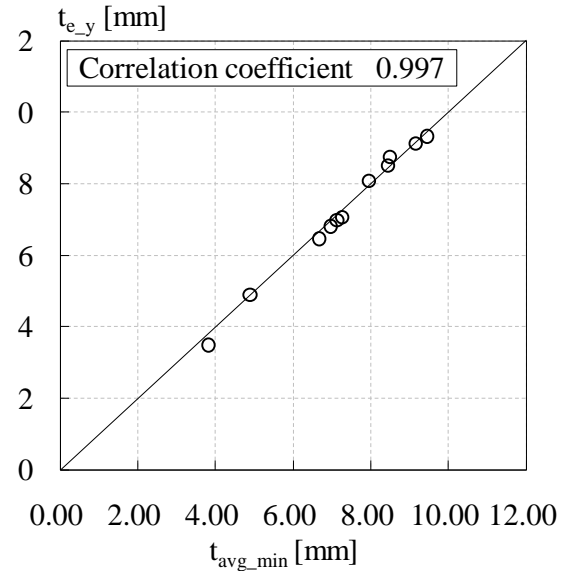
(a) Average thickness t_{avg}
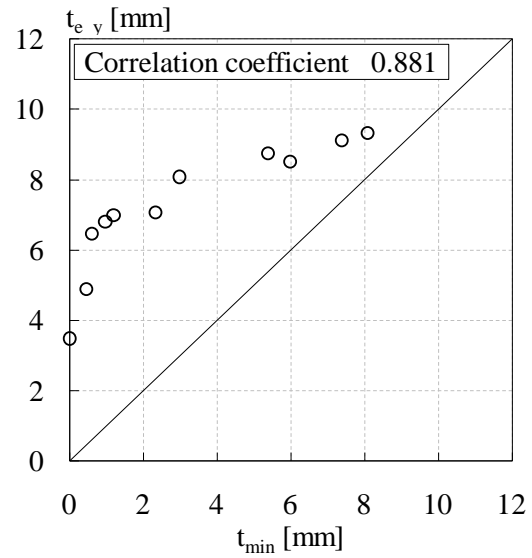
(b) Minimum thickness t_{min}
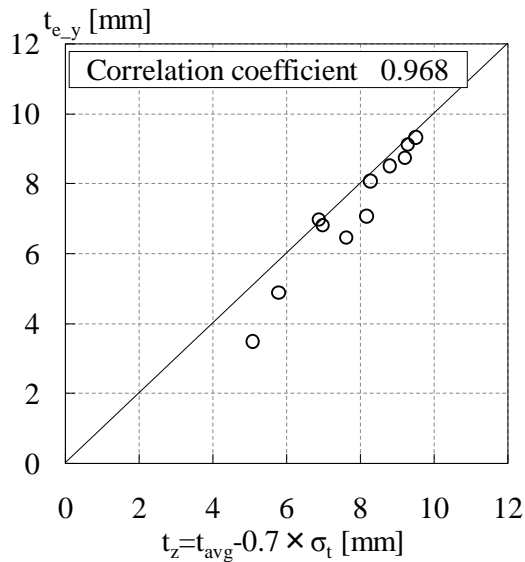
(c) $t_z = t_{avg} - 0.7\sigma_t$

(d) Minimum average thickness t_{avg_min}

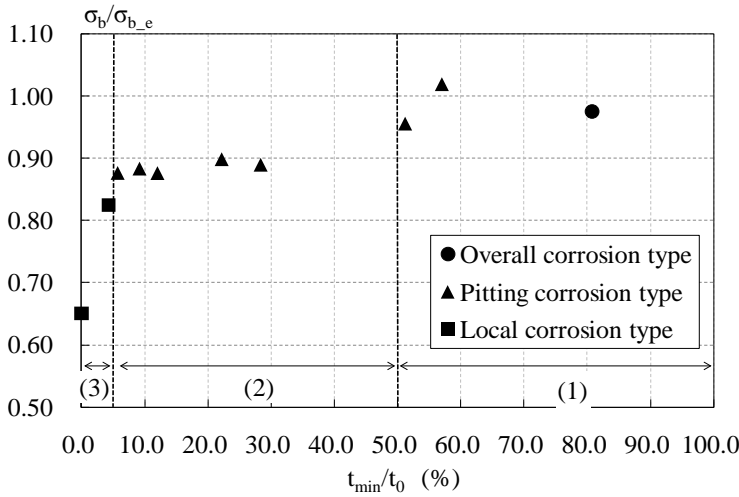**Figure9**. Correlation diagrams of effective thickness (yield strength)

proposed by Muranaka et al. (1998) from corroded tensile coupon tests. This thickness parameter has high correlation coefficient comparatively, but the overestimated result may be provided in the case of severe corroded plates for wide steel specimens.

From **Figure9** (d), the effective thicknesses are almost the same to minimum average thickness t_{avg_min}. Therefore, it thought that t_{avg_min} should be applied to effective thickness for the yield strength estimation with good accuracy. And the influence of stress concentration due to corrosion will be able to consider only by minimum section for yield strength.

5.2 Tensile strength estimation

From **Figure6**, since the stress concentration will occur significantly after yield load stage, it will be necessary that the effective thickness different from the yield strength estimation is investigated for the tensile strength. So, in this section, the correlations between an effective thickness and 4 statistical thickness parameters were investigated for tensile strength in a similar way to previous section.

Figure10 shows the correlation diagrams between an effective thickness of tensile strength (t_{e_b}) and

Figure11. σ_b/σ_{b_e} - t_{min}/t_0 relationship

Figure10. Correlation diagrams of effective thickness (tensile strength)

t_{avg_min}. The estimation results of other 3 thickness parameters were omitted from this section, because it cannot be found significant features from the tensile strength estimation results. In **Figure10**, applying t_{avg_min} to tensile strength estimation can obtain the high correlation coefficient (0.992) comparatively, but the overestimated result must be provided. As this reason, the stress concentration due to the surface irregularities will dominate the remaining strength at the ultimate state.

In this study, Form the consideration of breaking trigger point for Type-P and L, the improvement of effective thickness was tried by focusing attention on the remaining minimum thickness.
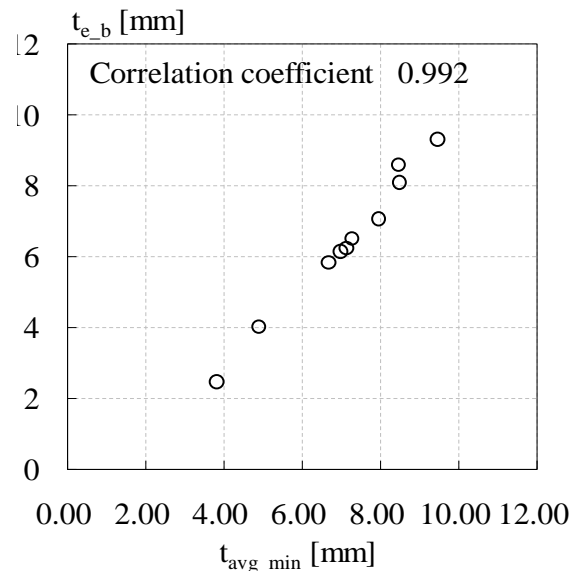
5.3 New effective thickness for tensile strength

In ultimate load stage, the crack occurring at severe corroded point will be dominated by the remaining thickness at minimum thickness point. So in this study, a new effective thickness as shown in (4.1) was proposed.

$$t_e = t_{avg\_min} \times \alpha \qquad (4.1)$$

Here, α: thickness reduction coefficient including the influence of minimum thickness. This thickness reduction coefficient α should be changed according to each corrosion type.

The relationship between the tensile strength ratio

(σ_b/σ_{b_e}) and the remaining minimum thickness ratio (t_{min}/t_0) is shown in **Figure11**. Here, σ_b: experimental result, σ_{b_e}: estimation result by using t_{avg_min}, t_0: initial thickness. In this figure, it can be confirmed that σ_b/σ_{b_e} is deteriorated with decreasing t_{min}/t_0. Especially, in the range of $t_{min}/t_0 \leqq 5.0\%$, σ_b/σ_{b_e} is significantly deteriorated. This fact means that the crack occurred at early load stage. On the other hand, in the range of $t_{min}/t_0 > 50\%$, σ_b/σ_{b_e} becomes almost 1.0. As the reason, it will mean that the breaking trigger become minimum section, not minimum thickness point. Finally, the t_{min}/t_0 was divided 3 regions (1)-(3) depending on σ_b/σ_{b_e}. And the value of σ_b/σ_{b_e} was applied to the thickness reduction coefficient ($\alpha = \sigma_b/\sigma_{b\_e}$). Namely, $t_{min}/t_0 > 50\%$: $\alpha = 1.0$, $5.0\% < t_{min}/t_0 \leqq 50\%$: $\alpha = 0.85$ and $t_{min}/t_0 \leqq 5.0\%$: $\alpha = 0.65$, respectively.

So, the correlation diagram between a new effective thickness of tensile strength (shown in Equation (4.1)) and effective thickness of experimental results is shown in **Figure12.** From this figure, it can be clarified that a new effective thickness parameter has the highest correlation with that based on experimental results. This result means that the remaining tensile strength of corroded plate will be able to estimate with good accuracy by using this
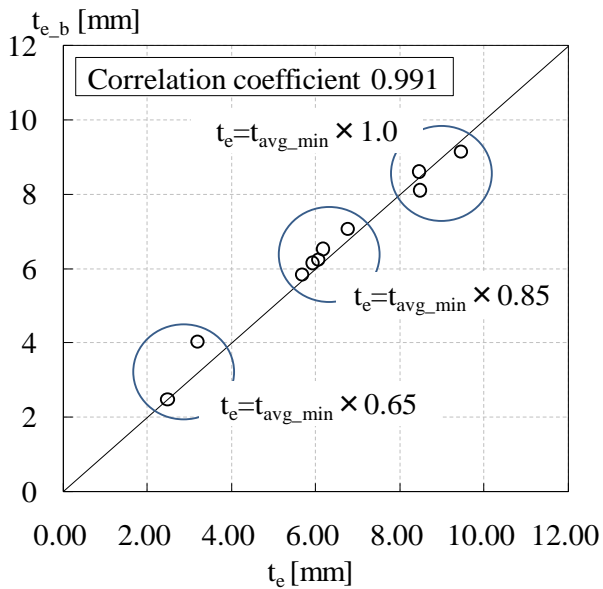
Figure12. New effective thickness for tensile strength

method, which was applied on not only the minimum average thickness but also the minimum thickness and its position.

In this paper, the experimental result about more severe corroded 11 specimens were reported, but the results of other 15 specimens also should be appended and reconsidered for this strength estimation method. And more experimental basal data by using actual size specimens should be accrued in near future.

6. CONCLUSIONS

The tensile test and steel surface measurement of severe corroded wide specimens were carried out in order to propose more accurate remaining strength estimation method for tensile corroded plates with actual member size. Main conclusions obtained from this study are as follows:

(1) Corroded surfaces were categorized to 3 typical corrosion types based on thickness measurement results.

(2) Influence of stress concentration due to surface irregularities appear clearly around yield load stage.

(3) If the local corrosion and large corrosion pits exist on plate surface, it should be focused attention on the remaining minimum thickness and its position as one of the breaking trigger.

(4) It thought that the minimum average thickness should be applied to effective thickness for the yield strength estimation with good accuracy.

(5) A simple estimation method, which used a thickness reduction coefficient including the minimum thickness, was proposed for the remaining tensile strength of severely corroded plates.

REFERENCES

Y. Fujino, E. Sasaki, Y. Suzuki, T. Nagayama, H. Hirayama and H. Nagatani, Talk-in on Maintenance of Steel Bridges in Japan, *Bridge and Foundation Engineering*, pp. 28-35, 2008.9. (In Japanese)

M. Matsumoto, N. Shiraishi and H. Miyake, The study on assessment of corrosion deterioration of steel bridges, *Journal of Structural Engineering*, Vol.38A, pp.1097-1102, 1992.4. (In Japanese)

A. Muranaka, O. Minata and K. Fujii, Estimation of residual strength and surface irregularity of the corroded steel plates, *Journal of Structural Engineering*, pp 19-25, Vol. 44A, pp.1063-1071, 1998.4. (In Japanese)

K. Tagaya, A. Kariya, T. Kaita, K. Fujii, T. Hara and M. Uenoya, Fundamental study on shear strength of corroded plate girder web, *Collaboration and Harmonization in Creative Systems (Proceedings of ISEC-03)*, Tokuyama, pp.99-104, 2005.9.

ACKNOWLEDGMENT